

Exosomal microRNA-618 derived from mesenchymal stem cells attenuate the progression of hepatic fibrosis by targeting Smad4

Chao Sun, Cuicui Shi, Xiaoyan Duan, Yi Zhang, and Baocan Wang

Department of Gastroenterology, Xin Hua Hospital Affiliated to Shanghai Jiao Tong University School of Medicine, Shanghai, China

ABSTRACT

Hepatic fibrosis (HF) is a pathological phenomenon that occurs during the process of long-term damage and repair in the liver. This condition will lead to the development of cirrhosis and even liver cancer if untreated. Previous evidence has shown that exosomes derived from mesenchymal stem cells (MSCs), carrying microRNAs (miRs), can affect the pathogenesis of HF. Therefore, the present study aimed to identify novel exosomal miRs derived from MSCs that play a critical role in the progression of HF. Next, the expression data of differentially expressed miRs (DEMs) of patients with liver cirrhosis and healthy controls were obtained from the Gene Expression Omnibus dataset. DEMs were analyzed using Gene ontology (GO) and Kyoto Encyclopedia of Genes and Genomes (KEGG). Moreover, to further confirm the function of exosomal miR-618 derived from MSCs on the pathogenesis of HF *in vivo*, a mouse model of HF was established. The results of the present study suggested that a close associated existed between DEMs and HF. Based on the results of the bioinformatics analysis, miR-618 was one of the main downregulated miRs involved in cirrhosis. In addition, miR-618 could be transferred from MSCs to LX-2 cells via exosomes; exosomal miR-618 derived from MSCs inhibited the viability and migration of LX-2 cells that were treated with TGF- β . Furthermore, exosomal miR-618 derived from MSCs attenuated the progression of HF via targeting Smad4. These findings indicated that treatment of exosomal miR-618 derived from MSCs might serve as a new strategy for HF.

ARTICLE HISTORY

Received 14 October 2021
Revised 22 December 2021
Accepted 23 December 2021

KEYWORDS

Hepatic fibrosis; cirrhosis;
miR-618; Smad4; exosomes

Introduction

Hepatic fibrosis (HF) is a pathological phenomenon produced in the process of long-term damage and repair in the liver [1,2]. During the formation of HF, hepatocytes are damaged by various factors, such as chronic liver disease, and excessive intake of alcohol, and secrete a variety of cytokines [3]. Subsequently, cytokines can stimulate the transformation of hepatic stellate cells into fibroblasts, resulting in excessive accumulation of extracellular matrix (ECM) in the liver [3]. Moreover, excessive accumulation of ECM leads to the formation of fibrous scarring, known as HF [4]. Finally, HF can further develop into cirrhosis and liver cancer, which seriously affect the health and life of patients [1]. However, to date, the application of an effective treatment for HF has not been reported [5]. The main treatment strategy is to prevent liver damage and to arrest or even reverse the progression of HF to cirrhosis [6].

Therefore, it is imperative to explore new treatment strategies for HF.

MicroRNAs (miRs) are a class of non-coding small RNAs, which can regulate gene expression [7]. miRs play a variety of roles during the growth and development of hepatocytes [8–10]. For instance, miR-30a prevents the progression of HF by inhibiting cell autophagy in a mouse model of HF [11]. Besides, miR-200a could significantly inhibit the progression of HF [12]. Moreover, miR-378 promoted the progression of HF by up-regulating the NF- κ B pathway [13]. In the present study, a Gene Expression Omnibus (GEO) dataset was used to identify differentially expressed miRs (DEMs) by comparing the expression profile of miRs between patients with liver cirrhosis and healthy control subjects.

Mesenchymal stem cells (MSCs) are a type of pluripotent stem cells [14]. MSCs function by secreting a variety of cytokines that act on other cells [15]. Exosomes are small vesicles with

a diameter of 40–100 nm, which contain complex RNA, proteins and immunomodulatory factors [16]. Exosomes derived from MSCs can play tissue repair and immunomodulatory roles similar to those of MSCs [15–17]. In addition, they can deliver complex RNA molecules, proteins, or immunomodulatory factors, and play an important role in the development of different diseases [18]. For example, Chen *et al* indicated that exosomal miR-223 separated from MSCs could protect the liver against autoimmune hepatitis-caused injury [19]. In addition, it has been reported that exosomal miR-181-5p derived from MSCs can suppress the process of HF by activating autophagy [20]. The present study explored the key miRs, which play an anti-HF effect role firstly. We aimed to deliver these anti-HF miRs to the liver by exosomes and investigated their potential anti-HF effects.

Materials and methods

Clinical sample collection

The serum samples of five patients with liver cirrhosis and five healthy control subjects were collected from XinHua Hospital Affiliated to Shanghai Jiao Tong University School of Medicine. The study was proved by Ethics Committee of Xin Hua Hospital Affiliated to Shanghai Jiao Tong University School of Medicine. The written informed consents have been obtained from patients and healthy donors.

Differentially expressed miRs (DEMs) analysis and bioinformatics

The DEM expression data derived from a dataset including patients with liver cirrhosis (LC) and healthy controls (GSE156347) were downloaded from the GEO (<https://www.ncbi.nlm.nih.gov/geo/>). We analyzed the DEMs between four patients with HBV-LC without bacterial infection and four healthy controls using with R language $P < 0.05$ ($-\log_{10}$ p-value > 1.3) and (\log_2 Fold Change) > 1.5 was applied for screening. Next, five databases (miRWalk, miRanda, miRDB, RNA22, TargetsCan) were used to predict the target genes of DEMs [21]. Then, Gene ontology (GO) and Kyoto Encyclopedia of Genes and

Genomes (KEGG) enrichment analysis was conducted to analyze the potential functions and significant pathways of the protein targets of DEMs [22].

Cell culture

Bone MSCs and human hepatic stellate cell lines (LX-2) were purchased from Procell Life Science & Technology Co. Ltd. (Wuhan, Hubei, China). The cells were cultured in DMEM (Thermo Fisher Scientific, Inc. Waltham, MA, USA) medium supplemented with 10% fetal bovine serum (FBS) (Thermo Fisher Scientific, Inc.) and 1% penicillin and streptomycin (Thermo Fisher Scientific, Inc.) at 37°C in the presence of 5% CO₂. To mimic HF *in vitro*, LX-2 cells were exposed to TGF- β (5 ng/ml) for 24 h [23].

Cell transfection

MiR-618 agomir, miR-618 antagomir and miR-618 agomir negative control (NC, agomir-ctrl) were obtained from GenePharma (Shanghai, China). MiR-618 agomir or agomir-ctrl was transfected into MSCs using Lipofectamine® 2000 (Thermo Fisher Scientific, Inc.) [24]. The sequences of miR-618 agomir, miR-618 antagomir (anti-miR-618) and negative control (NC) were listed as follow: miR-618 agomir: 5'-AAACUCUACUUGUCCUUCUGAGU-3'; miR-618 antagomir: 5'-ACUCAGAAGGACAAGUAGAGUUU-3'; NC: 5'-CAAACCTACGGAGTGGACACTCCTCA-3'.

Reverse transcription-quantitative polymerase chain reaction (RT-qPCR)

Initially, TRIzol® reagent (ELK Biotechnology, Wuhan, Hubei, China) was used for the separation of total RNA from the serum samples of patients with liver cirrhosis and healthy control subjects. MSCs or exosomes were also used for RNA extraction. Next, EntiLink™ 1st Strand cDNA Synthesis kit (EQ003; ELK Biotechnology) was used for miRNA reverse transcription. Meanwhile, EntiLink™ 1st Strand cDNA Synthesis kit (EQ002; ELK Biotechnology) was used for mRNA reverse transcription. Remarkably, the specific sequences

Table 1. The specific sequences of primers for miRNA reverse transcription.

Name	Primer sequences (5'-3')
miR-4433-3p	CTCAACTGGTGCCTGGAGTCGGCAATTCAGTTGAGATGTCCCA
miR-4649-5p	CTCAACTGGTGCCTGGAGTCGGCAATTCAGTTGAGCTCTGAGA
miR-4651	CTCAACTGGTGCCTGGAGTCGGCAATTCAGTTGAGGCCCGACC
miR-4463	CTCAACTGGTGCCTGGAGTCGGCAATTCAGTTGAGGGCCCCAC
miR-4281	CTCAACTGGTGCCTGGAGTCGGCAATTCAGTTGAGCCCCCTC
miR-618	CTCAACTGGTGCCTGGAGTCGGCAATTCAGTTGAGACTCAGAA
miR-1273 c	CTCAACTGGTGCCTGGAGTCGGCAATTCAGTTGAGGACAGGGT
miR-4491	CTCAACTGGTGCCTGGAGTCGGCAATTCAGTTGAGTTTGGTCA
miR-3926	CTCAACTGGTGCCTGGAGTCGGCAATTCAGTTGAGTCTCTGCC
miR-4695-3p	CTCAACTGGTGCCTGGAGTCGGCAATTCAGTTGAGGAAGGAGG
U6	AACGCTTCACGAATTTGCGT

of primers for miRNA reverse transcription were shown in Table 1. In the meanwhile, oligo(dT) was used for mRNA reverse transcription. Then, EnTurbo™ SYBR Green PCR SuperMix (ELK Biotechnology) was used to perform qPCR. The $2^{-\Delta\Delta C_q}$ method was used for data comparison and analysis. U6 was employed as an endogenous control for miRNA. β -actin was worked as an endogenous control for Smad4 [25]. The sequences of the primers for real-time quantitative PCR used were shown in Table 2.

Isolation and identification of exosomes

The supernatant of MSC cells was transferred into a 15 ml centrifuge tube. The cell supernatant was centrifuged at 2,000 x g and 4°C for 30 min. Subsequently, the centrifuged samples were filtered with a 0.22- μ m membrane. Total Exosome Isolation reagent (Invitrogen, Thermo Fisher Scientific, Inc.; Carlsbad, CA, USA) was added to the supernatant sample. The samples were rotated and mixed evenly for 30 min, followed by centrifugation at 10,000 x g and 25°C for 10 min. Finally, exosome sediments were collected. Bicinchoninic acid (BCA) was used to detect the concentration of exosomes derived from MSCs. Nanoparticle Tracking Analysis (NTA) was used to detect the size distribution of the exosomes. Transmission Electron Microscopy (TEM) was used to observe the morphology of exosomes accordingly [26].

Exosome labeling and uptake

MSC Exo (exosomes derived from MSCs) or MSC^{miR-618 agomir} Exo (exosomes derived from

Table 2. The sequences of the primers for real-time quantitative PCR.

Name		Primer sequences (5'-3')
miR-4433-3p	Forward	GGACAGGAGTGGGGGTG
	Reverse	CTCAACTGGTGTCTGGAGTC
miR-4649-5p	Forward	GCGAGGGGTGGGCTCT
	Reverse	CTCAACTGGTGTCTGGAGTC
miR-4651	Forward	TTCGGGGTGGGTGAGGTC
	Reverse	CTCAACTGGTGTCTGGAGTC
miR-4463	Forward	GGCCGAGACTGGGGTG
	Reverse	CTCAACTGGTGTCTGGAGTC
miR-4281	Forward	GGGGGTCCCGGGGAG
	Reverse	CTCAACTGGTGTCTGGAGTC
miR-618	Forward	CGGGAAACTTACTTGTCTTC
	Reverse	CTCAACTGGTGTCTGGAGTC
miR-1273 c	Forward	GGGGGACAAAACGAGAC
	Reverse	CTCAACTGGTGTCTGGAGTC
miR-4491	Forward	GGCAATGTGGACTGGTGTG
	Reverse	CTCAACTGGTGTCTGGAGTC
miR-3926	Forward	GTGGCCAAAAGCAGGC
	Reverse	CTCAACTGGTGTCTGGAGTC
miR-4695-3p	Forward	GGTGATCTCACCCTGCC
	Reverse	CTCAACTGGTGTCTGGAGTC
Smad4	Forward	CCTCCATTTCCAATCATCT
	Reverse	CAGAAGGGTCCACGTATCCATC
U6	Forward	CTCGCTTCGGCAGCACAT
	Reverse	AACGCTTCACGAATTTGCGT
β -actin	Forward	GTCCACCGCAAATGCTTCTA
	Reverse	TGCTGTACCTTCACCGTTC

MSCs that were treated with miR-618 agomir) were labeled with PKH26. Subsequently, LX-2 cells were incubated with PKH26-labeled exosomes. The nuclei or the cytoskeletons were stained using DAPI or phalloidin dye, respectively [26]. Subsequently, fluorescence microscopy was applied to observe the stained images.

Western blot analysis

Total protein was harvested from exosomes or LX-2 cells with RIPA lysis buffer (Aspen, Wuhan, Hubei, China). The BCA protein assay kit (Aspen) was used to measure the concentration levels of the proteins.

Subsequently, the proteins were separated by SDS-PAGE (10%), transferred to PVDF membranes and immunoblotted with primary antibodies at 4°C overnight. The antibodies for CD81 (1:1,000; cat. no. ab109201), collagen I (1:1,000; cat. no. ab260043), α -SMA (1:1,000; cat. no. ab124964), Smad4 (1:1,000; cat. no. ab40759; Abcam, Cambridge, MA, USA), TSG101 (1:1,000; cat. no. 14,497-1-AP; Proteintech Group, Inc., Wuhan, Hubei, China), and β -actin (1:10,000; cat. no. TDY051; Beijing TDY Biotech Co., Ltd., Beijing, China) were used for detection of the corresponding proteins. Subsequently, the membranes were incubated with a corresponding secondary antibody (1:5,000; cat. no. AS1107; Aspen) at room temperature for 1 h. Subsequently, enhanced chemiluminescence was used to visualize the immunoreactive proteins [25].

Cell counting kit-8 (CCK-8) assay

LX-2 cells were seeded into 96-well plates and cultured overnight. The cells were incubated with 10 μ l CCK-8 solution (Dojindo, Kumamoto, Japan) for 2 h at 37°C. A microplate reader was used to measure the optical density at 450 nm [27].

Wound healing assay

The wound healing assay was performed to detect the wound healing activity of LX-2 cells. LX-2 cells were seeded into six-well plates. When LX-2 cells reached 100% fusion, scratches were made in each well with sterile 10 μ l pipette tips. Subsequently, microscopy was used to obtain the relevant images following scratching [28].

Transwell migration assay

LX-2 cells were placed on the upper chamber (Corning, NY, USA) containing 200 μ l serum-free DMEM. In addition, the lower chambers contained 600 μ l DMEM supplemented with 10% FBS. Following 24 h of incubation at 37°C, the cells were stained with 0.1% crystal violet on the lower surface. Microscopy was performed to observe the stained LX-2 cells [29].

Dual-luciferase reporter assay

LX-2 cells were co-transfected with the pGL6-miR-based luciferase reporter plasmids (Beyotime, Beijing, China) containing wild-type (WT) or mutant (MT) 3'-UTR of Smad4, together with miR-618 agomir or miR-618 agomir-control using Lipofectamine® 2000. The Dual Luciferase Reporter Assay System (Beyotime Institute of Biotechnology, Beijing, China) was used to detect luciferase activity in LX-2 cell lysates [30].

RNA pull-down assay

The RNA pull-down assay was performed using Pierce Magnetic RNA-Protein Pull-Down Kit (Thermo Fisher Scientific, Inc.). The RNA structure buffer (Thermo Fisher Scientific, Inc.) induced the formation of secondary structures in biotin-labeled RNAs. Subsequently, streptavidin-conjugated magnetic beads were incubated with biotin-labeled RNAs and the lysates from LX-2 cells were added to the complex and rotated for 1 h. Subsequently, the mixture was separated to obtain biotin-labeled miR-618 probe-protein-streptavidin-conjugated magnetic beads. Finally, RNA was isolated from the magnetic beads and RT-qPCR was performed to measure the expression levels of miR-618 [31].

In vivo model of HF

C57BL/6 J mice were provided by the Chinese Academy of Sciences (Shanghai, China). All animal procedures were approved by the Ethics Committee of XinHua Hospital Affiliated to Shanghai Jiao Tong University School of Medicine. The National Institutes of Health Guide for the Care and Use of Laboratory Animals was strictly followed. Initially, CCl₄ was dissolved in olive oil, at a ratio of 1:10. Moreover, C57BL/6 J mice were randomized into four groups as follows: Control, CCl₄, CCl₄ (4 weeks), CCl₄ (8 weeks), and CCl₄ (8 weeks) + MSC^{miR-618 agomir} Exo. The mice were intraperitoneally injected with 0.5 mg/kg CCl₄ for a maximum period of 4 or 8 weeks twice a week. The mice in the CCl₄ (8 weeks) + MSC^{miR-618 agomir} Exo group were injected with MSC^{miR-618 agomir} Exo (10 mg/kg)

at 2 days before the first CCl₄ treatment via the tail vein. In addition, the animal's activity, mental state, and diet were observed. Subsequently, the mice were sacrificed and liver tissues were collected at the end of the study [20,32].

Hematoxylin and eosin (H&E) staining

The liver tissues of the mice were separated and embedded in paraffin. Subsequently, the slices were stained with hematoxylin for 20 min followed by eosin staining for 10 sec. The stained tissues were observed using microscopy [12].

Masson staining

The liver tissues of the mice were separated and embedded in paraffin. Subsequently, the slices were nucleated with Regaud hematoxylin for 10 min. The tissues were stained with Masson Ponceau S acidic solution for 10 min and differentiated with 1% phosphomolybdate aqueous solution for 5 min. The stained tissues were observed using microscopy [12].

Detection of important indicators of liver lesions

The levels of alanine aminotransferase (ALT) and aspartate aminotransferase (AST) were detected using the corresponding kits (Alanine aminotransferase and Aspartate aminotransferase Assay Kits) according to the manufacturer's instructions [33]. The ALT Assay Kit and the AST Assay Kit were provided by Nanjing Jiancheng Bioengineering Institute (Nanjing, Jiangsu, China).

Immunohistochemical staining

The liver tissues of the mice were fixed in 4% paraformaldehyde, embedded in paraffin, and cut into 5 µm-thick slices. Subsequently, the tissues were soaked in xylene three times for 10 min each. The tissues were gradually soaked in 100%, 95%, 85%, and 70% ethanol for 5 min and incubated with primary antibodies against α-SMA and Smad4 (anti-α-SMA and anti-Smad4) at 4°C overnight. The following day, the samples were incubated with HRP-labeled secondary antibodies at 37°C for 30 min. Subsequently, 3,3'-

diaminobenzidine was added to the slices for color development. Finally, the stained tissues were observed using fluorescence microscopy [20]. The primary and secondary antibodies were obtained from Abcam.

Statistical analysis

The data were analyzed using GraphPad Prism version 7.0 (GraphPad Software, La Jolla, CA, USA) and expressed as mean ± SD. The differences were compared using ANOVA and Tukey's tests. P < 0.05 was considered to indicate a statistically significant difference [30].

Results

Identification of DEM expression between patient with liver cirrhosis and healthy control

It has been reported that miRs play a crucial role during the growth of hepatocytes [8–10]. To explore the potential of miRs to affect the development of cirrhosis in the tissues, R language was used to screen for DEMs from the GEO dataset using the accession number GSE156347. Following analysis of the DEM expression between patients with liver cirrhosis and healthy subjects, DEMs (upregulated and downregulated miRs) were identified in the GSE156347 dataset (Figure 1(a)). In addition, Volcano plot was used to display these DEMs (Figure 1(b)). The top five unregulated miRs were hsa-miR-4433-3p, hsa-miR-4649-5p, hsa-miR-4651, hsa-miR-4463 and hsa-miR-4281; the top five downregulated miRs were hsa-miR-618, hsa-miR-1273 c, hsa-miR-4491, hsa-miR-3926 and hsa-miR-4695-3p.

Moreover, the result of RT-qPCR confirmed that the expressions of miR-4433-3p, miR-4649-5p, miR-4463 and miR-4281 in patient with liver cirrhosis were notably higher than those in healthy control (Figure 1(c)). Meanwhile, the levels of miR-618, miR-1273 c, miR-4491 and miR-4695-3p in patient with liver cirrhosis were remarkably lower than those noted in healthy control (Figure 1(c)). Besides, the expression of miR-4651 and miR-3926 in patient with liver cirrhosis were not significantly different from those in healthy control (Figure 1(c)). The data suggested

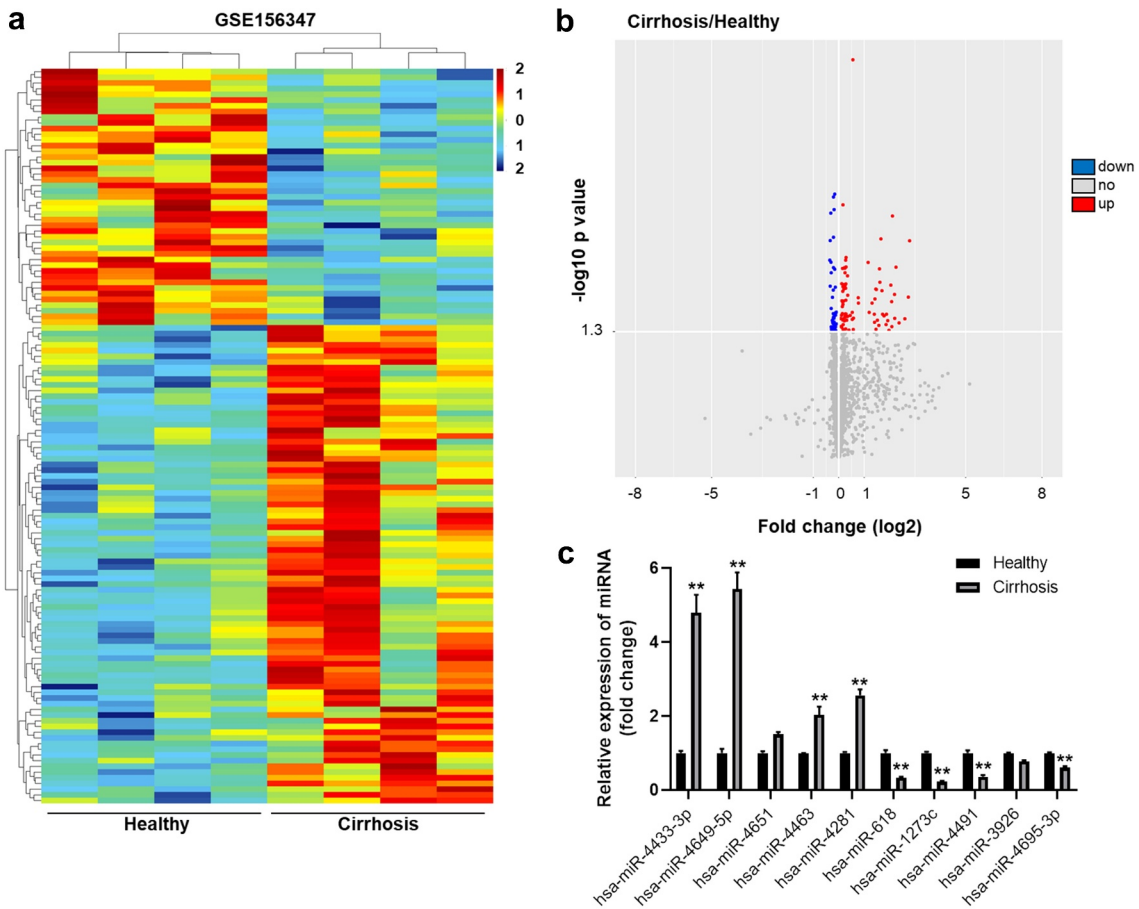


Figure 1. Identification of DEMs expression between liver cirrhosis tissues and healthy controls. (a) Heat map of DEMs in GSE156347 dataset. (b) Volcano plot of DEMs in GSE156347. The red spots represented upregulated miRNAs. The blue spots represented downregulated miRNAs. (c) RT-qPCR was performed to detect the expressions of miR-4433-3p, miR-4649-5p, miR-4651, miR-4463, miR-4281, miR-618, miR-1273 c, miR-4491, miR-3926 and miR-4695-3p in the serum samples of patients with liver cirrhosis and healthy control subjects. **P < 0.01 compared with control group, n = 3.

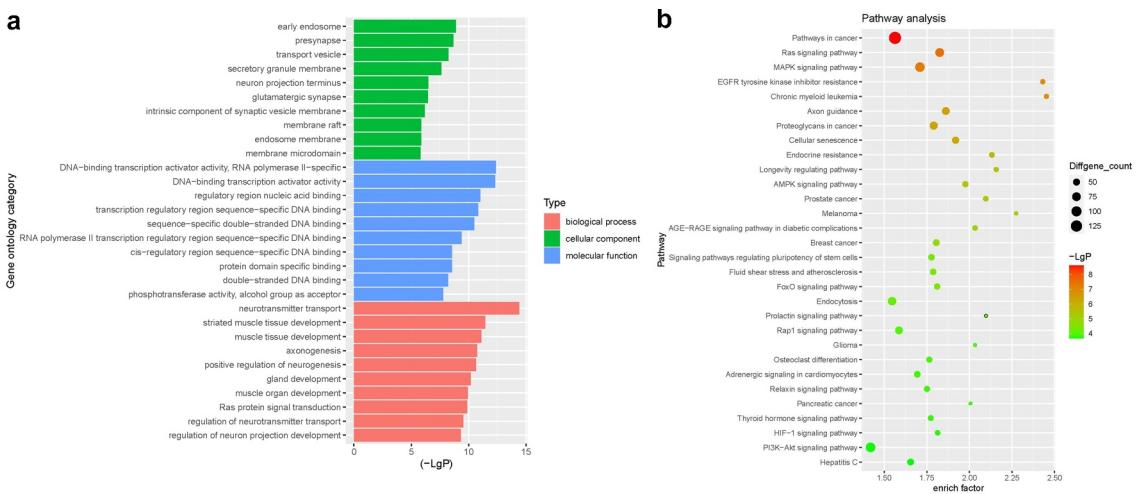


Figure 2. GO enrichment and KEGG pathway analyses. (a) GO enrichment analysis was used to analyze the functional information associated with DEMs. (b) KEGG pathway analysis was used to analyze the functional information associated with DEMs.

the identification of DEM expression between patient with liver cirrhosis and healthy control.

GO enrichment and KEGG pathway analyses

To analyze the functional information associated with DEMs, GO and KEGG enrichment analyses were performed. As shown in Figure 2(a), DEMs were mainly involved in ‘neurotransmitter transport’ and ‘striated muscle tissue development’ (Figure 2(a)). In addition, KEGG analysis results revealed that the target proteins of DEMs were mainly involved in the ‘pathways associated in cancer’, ‘Ras signaling pathway’, ‘MAPK signaling pathway’ and ‘PI3K-Akt signaling pathway’ (Figure 2(b)).

MiR-618 is transferred from MSCs to LX-2 cells via exosomes

We next explored the key miRNA involve in the progression of HF. Based on the results of the bioinformatics analysis and RT-qPCR, miR-618 was identified as one of the significantly down-regulated miRs in cirrhosis. In addition, it has

been reported that miR-618 plays an important role in the pathogenesis and progression of hepatopathy [34]. Therefore, the current study focused on investigating the function of miR-618 in liver fibrosis. To confirm the expression levels of miR-618 in cirrhotic tissues, RT-qPCR analysis was performed. As indicated in Figure 3(a), the expression levels of miR-618 in patient with cirrhotic were significantly lower than those noted in healthy control tissues. Moreover, by performing literature search, it was deduced that exosomal miRs derived from MSCs could suppress the process of HF [20]. Subsequently, the present study investigated whether miR-618 could be transferred from MSCs to LX-2 cells via exosomes. RT-qPCR analysis indicated that miR-618 agomir caused a significant upregulation in the levels of miR-618 in MSCs, compared with those of the control group (Figure 3(b)). Subsequently, exosomes were derived from MSCs (MSC Exo) or MSCs that were treated with miR-618 agomir (MSC^{miR-618 agomir} Exo). NTA results indicated that the diameters of these vesicles ranged from 50–150 nm (Figure 3(c)), and that the exosomal specific surface biomarkers CD81 and TSG101 were also detected (Figure 3(d)). Moreover, the results of TEM

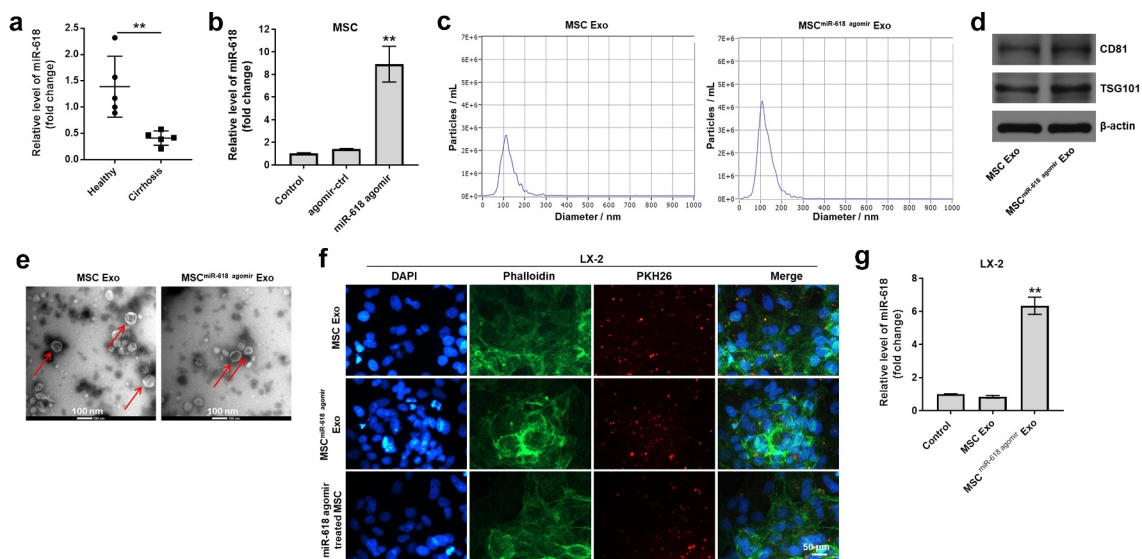


Figure 3. MiR-618 could be transferred from MSCs to LX-2 cells via exosomes. (a) RT-qPCR was performed to detect the expression of miR-618 from the serum samples of patients with liver cirrhosis and healthy control subjects. (b) RT-qPCR was performed to detect the expression of miR-618 in MSCs. (c) NTA was performed to detect the diameters of these vesicles. (d) Western blot assay was performed to detect the expression of exosomal markers CD81 and TSG101. (e) TEM was performed to observe the morphology of exosomes. (f) PKH26-labeled exosomes that were derived from MSCs could be internalized by LX-2 cells. These results were observed using a fluorescence microscope. Blue color: LX-2 cell nucleus; green color: LX-2 cells; red color: exosome. (g) RT-qPCR was performed to detect the expression of miR-618 in LX-2 cells. ** $P < 0.01$ compared with control group, $n = 3$.

analysis indicated that these vesicles were cup-shaped and round (Figure 3(e)). In conclusion, these results confirmed that the vesicles derived from MSCs were exosomes.

Subsequently, to assess whether exosomes derived from MSCs could be internalized by LX-2 cells, the latter cells were incubated with exosomes that were labeled with the PKH26 dye. The results revealed that this dye could be observed in LX-2 cells, suggesting that MSC-derived exosomes could be absorbed by these cells (figure 3(f)). The levels of miR-618 in LX-2 cells that were treated with MSC^{miR-618} agomir Exo were significantly higher than those noted in LX-2 cells that were treated with MSC Exo (Figure 3(g)). In addition, miR-618 agomir-treated MSCs had been co-cultured with LX-2 cells and the outcome suggested MSC-derived exosomes could be absorbed

by cells as well (figure 3(f)). Taken together, these data indicated that miR-618 could be transferred from MSCs to LX-2 cells via exosomes.

Exosomal miR-618 derived from MSCs inhibits the viability and migration of LX-2 cells treated with TGF- β

To mimic the progression of HF *in vitro*, LX-2 cells were treated with 5 ng/ml TGF- β . The ability of exosomal miR-618 to affect the viability of LX-2 cells was investigated using the CCK-8 assay. The results indicated that TGF- β significantly promoted the viability of LX-2 cells; however, this phenomenon was reversed in the MSC^{miR-618} agomir Exo group (Figure 4(a)). In contrast, MSC^{anti-miR-618} Exo notably enhanced the effect of TGF- β on the proliferation of LX-2 cells (Figure 4(a)). In addition,

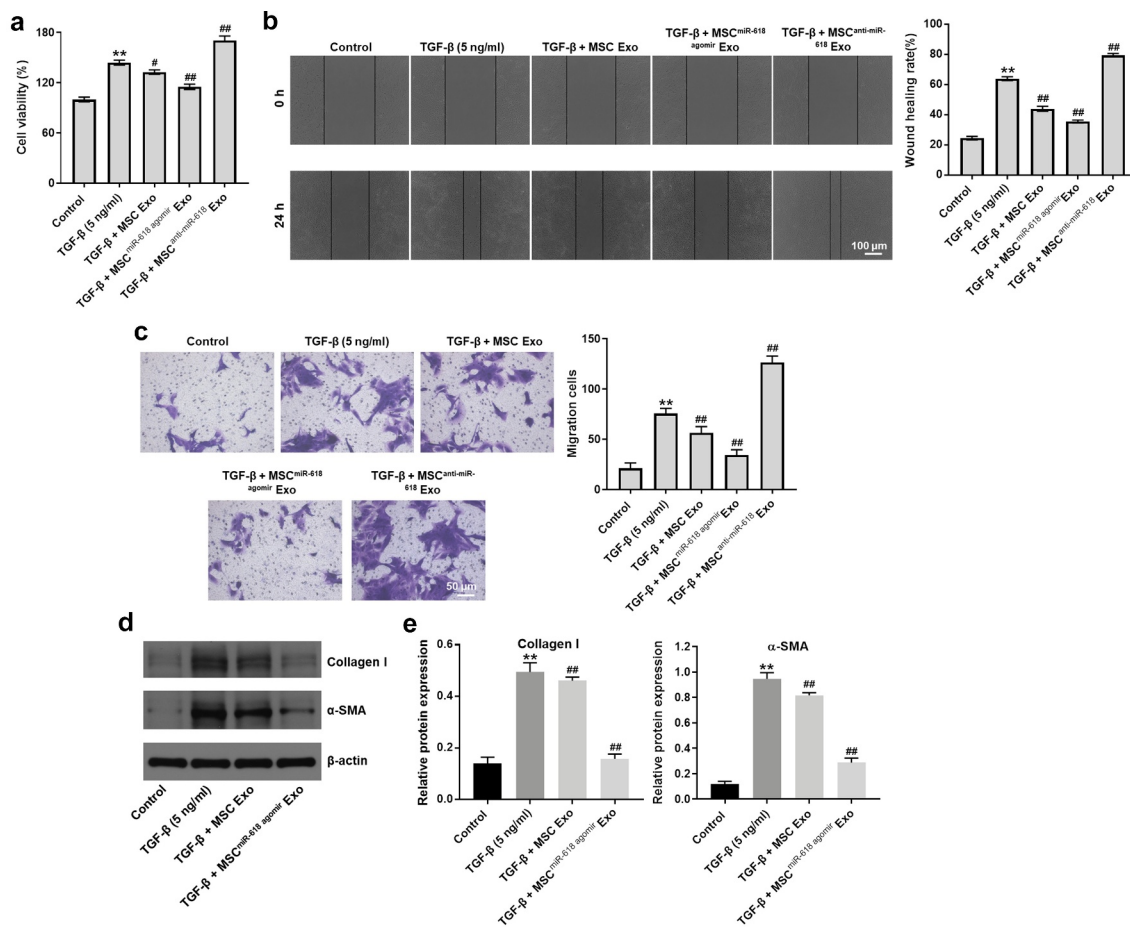


Figure 4. Exosomal miR-618 derived from MSCs could inhibit the viability and migration of LX-2 cells that were treated with TGF- β . (a) CCK-8 assay was performed to detect the viability of LX-2 cells. (b) Wound healing assay was performed to detect the migration ability of LX-2 cells. (c) Transwell assay was performed to detect the migration ability of LX-2 cells. (d, e) Western blot assay was performed to detect the expression of Collagen I and α -SMA in LX-2 cells. ** $P < 0.01$ compared with control group; # $P < 0.01$, ## $P < 0.01$, compared with TGF- β group, $n = 3$.

the results of the wound healing and transwell assays indicated that TGF- β notably promoted the migratory ability of LX-2 cells compared with that of the control group; however, the effects of TGF- β were reversed following treatment of the cells with MSC^{miR-618 agomir} Exo (Figure 4(b) and (c)). Meanwhile, MSC^{anti-miR-618} Exo enhanced the effect of TGF- β on cell migration (Figure 4(b) and (c)). As expected, TGF- β caused a notable upregulation in the expression levels of collagen I and α -SMA in LX-2 cells compared with those noted in the control group, while this increase was inhibited by MSC^{miR-618 agomir} Exo (Figure 4(d) and (e)). These data suggested that exosomal miR-618 derived from

MSCs inhibited the viability and migration of LX-2 cells pre-treated with TGF- β .

Smad4 is targeted and negatively regulated by miR-618

In order to predict the alternative binding targets of miR-618, Targetscan, and miRWalk online databases were used. Database analysis suggested that Smad4 may be one of the potential targets of miR-618 (Figure 5(a)). In addition, Smad4 was closely associated with the progression of HF [35,36]. Therefore, Smad4 was selected for

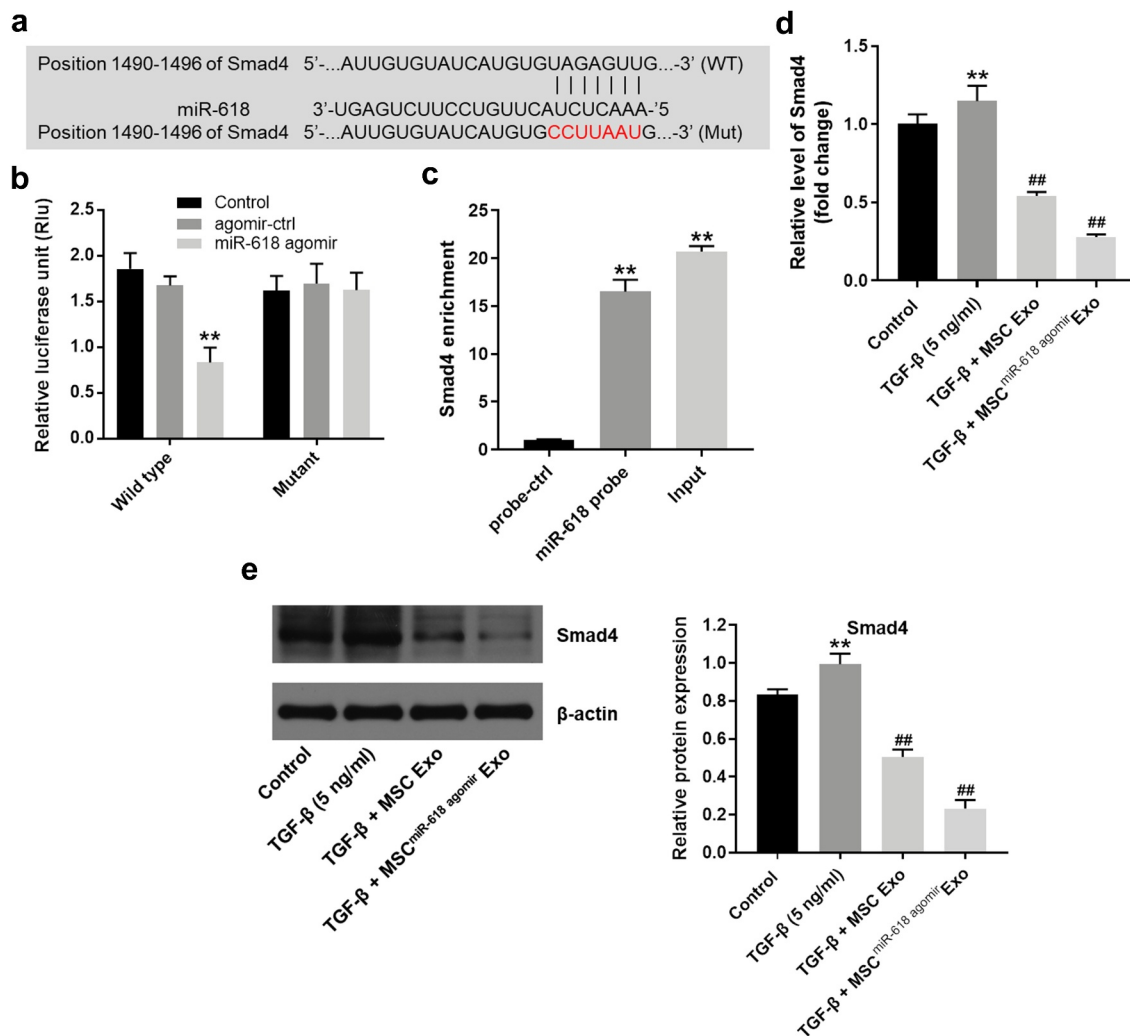


Figure 5. Smad4 is targeted and negatively regulated by miR-618. (a) Sequence alignment of miR-618 with the binding sites within the WT or MT regions of Smad4. (b) Dual-luciferase reporter assay was used to confirm the binding of miR-618 and Smad4 in LX-2 cells. (c) RNA pull-down assay exhibited the interaction of miR-618 and Smad4 in LX-2 cells. (d) RT-qPCR was performed to detect the expression of Smad4 in LX-2 cells. (e) Western blot assay was performed to detect the expression of Smad4 in LX-2 cells. **P < 0.01 compared with control group; ##P < 0.01, compared with TGF- β group, n = 3.

investigation in the subsequent experiments. Dual-luciferase reporter assay indicated that the luciferase activity of LX-2 cells transfected with Smad4 WT was notably decreased by miR-618 agomir, while the luciferase activity of cells transfected with Smad4 MT was not affected (Figure 5(b)). Moreover, the results of the RNA pull-down assay suggested that miR-618 was directly binding to the mRNA of Smad4, which confirmed the interaction of miR-618 and Smad4 in LX-2 cells (Figure 5(c)).

The data indicated that TGF- β significantly increased the expression levels of Smad4 in LX-2 cells, compared with those of the control group. In contrast to these findings, MSC^{miR-618} agomir Exo markedly inhibited the expression levels of Smad4 in LX-2 cells that were treated with TGF- β

(Figure 5(d) and (e)). In summary, Smad4 was targeted and negatively regulated by miR-618.

Exosomal miR-618 derived from MSCs attenuates the progression of HF by targeting Smad4

Finally, to further confirm the function of MSC^{miR-618} agomir Exo during the pathogenesis of HF, an *in vivo* mouse model of HF was established. To observe the pathogenesis of HF *in vivo*, H&E and Masson staining were performed. As indicated in Figure 6(a), CCl₄ notably induced the formation of fibrosis in mouse tissues in a time-dependent manner, while MSC^{miR-618} agomir Exo treatment significantly alleviated the progression of HF. In addition, CCl₄ significantly increased the areas of liver

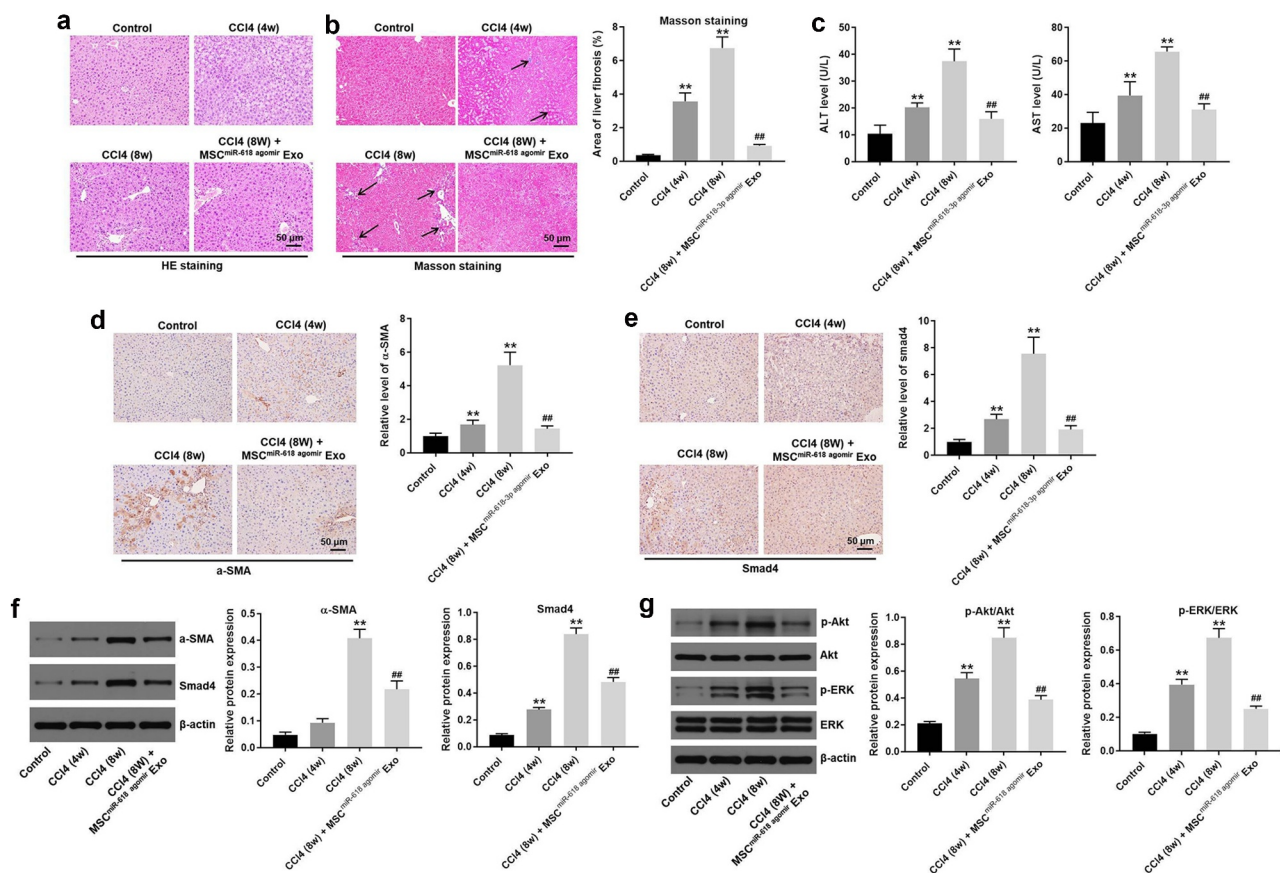


Figure 6. Exosomal miR-618 derived from MSCs attenuates the progression of HF by targeting Smad4. (a) HE staining was conducted to observe the tissues morphology of mouse. (b) Masson staining was conducted to observe the areas of liver fibrosis in mouse tissues (arrow points to fibrosis area). (c) The levels of ALT and AST were detected by Alanine aminotransferase Assay Kit and Aspartate aminotransferase Assay Kit. (d, e) IHC staining was conducted to detect the expressions of α -SMA and Smad4 in mouse tissues. (f, g) Western blot assay was performed to detect the expressions of α -SMA, Smad4, p-Akt and p-ERK in mouse liver tissues. ** $P < 0.01$ compared with control group; ## $P < 0.01$, compared with TGF- β group, $n = 3$.

fibrosis in mouse tissues, while this increase was reversed by MSC^{miR-618 agomir} Exo (Figure 6(b)). Moreover, CCl₄ caused a marked upregulation of the expression levels of ALT and AST; however, these effects were significantly inhibited by treatment with MSC^{miR-618 agomir} Exo (Figure 6(c)). Meanwhile, CCl₄ notably increased the expression levels of α -SMA and Smad4 in mouse liver tissues, while this increase was significantly reversed following treatment with MSC^{miR-618 agomir} Exo (Figure 6(d,e) and (f)). Furthermore, in order to verify results 1 and 2, relevant molecular biology experiments were performed. As indicated in Figure 6(g), CCl₄ significantly increased the expressions of p-Akt and p-ERK in mouse liver tissues; however, these increases were notably reversed by MSC^{miR-618 agomir} Exo. Collectively, the data indicated that exosomal miR-618 derived from MSCs could attenuate the development of HF by targeting Smad4.

Discussion

In the last decades, the identification of miRs carried by exosomes that have been derived from MSCs has become a popular research topic. miRs carried by exosomes derived from MSCs play an important role in the development of hepatocytes through various mechanisms [37,38]. For example, exosomal miRNA-23b derived from bone MSC is able to inhibit the inflammation of lipopolysaccharide (LPS)-induced BV2 inflammatory cells [39]. Besides, exosomal miR-122 originating from adipose tissue-derived mesenchymal stem cells (AMSCs) can significantly promote the induction of apoptosis of hepatocellular carcinoma cells [37]. In an analogous way, exosomal miR-199a derived from AMSCs can significantly increase the sensitivity of hepatocellular carcinoma cells to chemotherapeutic agents (doxorubicin) by inducing apoptosis [38]. In the present study, the results demonstrated that exosomal miR-618 derived from MSCs was able to inhibit the viability and migration of LX-2 cells that were treated with TGF- β . Our findings are consistent with previously reported results. All these results suggested that exosomal miR derived

from MSCs could be a promising treatment for liver diseases.

In addition, it has been shown that miR-618 plays an important role in the development of liver-related diseases [34]. In the present study, exosomal miR-618 derived from MSCs could attenuate the progression of HF by targeting Smad4. Initially, the exosomes were derived from MSCs and the expression levels of miR-618 were investigated in association with the pathogenesis of HF. The data indicated that miR-618 may be regarded as a potential therapeutic target.

TGF- β is one of the most important cytokines leading to the formation and progression of HF [40–42]. For example, miR-122 can inhibit TGF- β 1-induced EMT processes in LX-2 cells by down-regulating the TGF- β 1/Smad signaling pathway [41]. Besides, down-regulation of miR-486-5p alleviates oxidative stress injury in hepatocytes by inhibiting the TGF- β /Smad pathway [43]. In addition, overexpression of miR-210 can increase apoptosis of primary hepatocytes induced by hypoxia/reoxygenation (HR) by negatively regulating Smad4 [42]. In the current study, exosomal miR-618 derived from MSCs attenuated the progression of HF by negatively targeting Smad4, which was consistent with the aforementioned studies.

The current study exhibits certain limitations. For example, miR-618 plays an important role in the course of HF, while other related miRs require further investigation in future studies. In addition, the potential of exosomal miR-618 derived from MSCs to regulate other related signaling pathways in the development of HF requires further investigation.

Conclusion

In conclusion, exosomal miR-618 derived from MSCs attenuated the progression of HF by negatively targeting Smad4. The current study indicated that treatment of exosomal miR-618 derived from MSCs might serve as a new strategy for HF.

Ethics approval and consent to participate

All animal procedures were approved by Xin Hua Hospital Affiliated to Shanghai Jiao Tong University School of

Medicine. National Institutes of Health Guide for the Care and Use of Laboratory Animals was followed strictly. The written informed consents have been obtained from patients and healthy donors.

Disclosure statement

No potential conflict of interest was reported by the author(s).

Funding

The author(s) reported there is no funding associated with the work featured in this article.

Availability of data and materials

The datasets analyzed during the current study are available from the corresponding author on reasonable request.

References

- [1] Altamirano-Barrera A, Barranco-Fragoso B, Méndez-Sánchez N. Management strategies for liver fibrosis. *Ann Hepatol.* **2017**;16:48–56.
- [2] Parola M, Pinzani M. Liver fibrosis: pathophysiology, pathogenetic targets and clinical issues. *Mol Aspects Med.* **2019**;65:37–55.
- [3] Dawood RM, El-Meguid MA, Salum GM, et al. Key players of hepatic fibrosis. *J Interferon Cytokine Res.* **2020**;40:472–489.
- [4] Ezhilarasan D, Sokal E, Najimi M. Hepatic fibrosis: it is time to go with hepatic stellate cell-specific therapeutic targets. *HBPD INT.* **2018**;17:192–197.
- [5] Lambrecht J, van Grunsven LA, Tacke F. Current and emerging pharmacotherapeutic interventions for the treatment of liver fibrosis. *Expert Opin Pharmacother.* **2020**;21:1637–1650.
- [6] Fagone P, Mangano K, Pesce A, et al. Emerging therapeutic targets for the treatment of hepatic fibrosis. *Drug Discov Today.* **2016**;21:369–375.
- [7] Lu TX, Rothenberg ME. MicroRNA. *J Allergy Clin Immunol.* **2018**;141:1202–1207.
- [8] Fabian MR, Sonenberg N, Filipowicz W. Regulation of mRNA translation and stability by microRNAs. *Annu Rev Biochem.* **2010**;79:351–379.
- [9] Zhou Y, Ren H, Dai B, et al. Hepatocellular carcinoma-derived exosomal miRNA-21 contributes to tumor progression by converting hepatocyte stellate cells to cancer-associated fibroblasts. *J Exp Clin Cancer Res.* **2018**;37:324.
- [10] Heo MJ, Kim TH, You JS, et al. Alcohol dysregulates miR-148a in hepatocytes through FoxO1, facilitating pyroptosis via TXNIP overexpression. *Gut.* **2019**;68:708–720.
- [11] Chen J, Yu Y, Li S, et al. MicroRNA-30a ameliorates hepatic fibrosis by inhibiting Beclin1-mediated autophagy. *J Cell Mol Med.* **2017**;21:3679–3692.
- [12] Xu A, Zhong G, Wang J, et al. MicroRNA 200a inhibits liver fibrosis of schistosoma. *Bioengineered.* **2021**;12:4736–4746.
- [13] Zhang T, Hu J, Wang X, et al. MicroRNA-378 promotes hepatic inflammation and fibrosis via modulation of the NF- κ B-TNF α pathway. *J Hepatol.* **2019**;70:87–96.
- [14] Bianco P. “Mesenchymal” stem cells. *Annu Rev Cell Dev Biol.* **2014**;30:677–704.
- [15] Ullah I, Subbarao RB, Rho GJ. Human mesenchymal stem cells - current trends and future prospective. *Biosci Rep.* **2015**;35:e00191.
- [16] Yaghoubi Y, Movassaghpour A, Zamani M, et al. Human umbilical cord mesenchymal stem cells derived-exosomes in diseases treatment. *Life Sci.* **2019**;233:116733.
- [17] Fu X, Liu G, Halim A, et al. Mesenchymal stem cell migration and tissue repair. *Cells.* **2019**;8:784.
- [18] Harrell CR, Jovicic N, Djonov V, et al. Mesenchymal stem cell-derived exosomes and other extracellular vesicles as new remedies in the therapy of inflammatory diseases. *Cells.* **2019**;8:1605.
- [19] Chen L, Lu FB, Chen DZ, et al. BMSCs-derived miR-223-containing exosomes contribute to liver protection in experimental autoimmune hepatitis. *Mol Immunol.* **2018**;93:38–46.
- [20] Qu Y, Zhang Q, Cai X, et al. Exosomes derived from miR-181-5p-modified adipose-derived mesenchymal stem cells prevent liver fibrosis via autophagy activation. *J Cell Mol Med.* **2017**;21:2491–2502.
- [21] Lewis BP, Burge CB, Bartel DP. Conserved seed pairing, often flanked by adenosines, indicates that thousands of human genes are microRNA targets. *Cell.* **2005**;120:15–20.
- [22] Liu G, Lei Y, Luo S, et al. MicroRNA expression profile and identification of novel microRNA biomarkers for metabolic syndrome. *Bioengineered.* **2021**;12:3864–3872.
- [23] Feng Y, Wei G, Zhang L, et al. LncRNA DARS-AS1 aggravates the growth and metastasis of hepatocellular carcinoma via regulating the miR-3200-5p-Cytoskeleton associated protein 2 (CKAP2) axis. *Bioengineered.* **2021**;12:8217–8232.
- [24] Chen L, Zhu Q, Lu L, et al. MiR-132 inhibits migration and invasion and increases chemosensitivity of cisplatin-resistant oral squamous cell carcinoma cells via targeting TGF- β 1. *Bioengineered.* **2020**;11:91–102.
- [25] He S, Zhang W, Li X, et al. Oral squamous cell carcinoma (OSCC)-derived exosomal MiR-221 targets and

- regulates phosphoinositide-3-kinase regulatory subunit 1 (PIK3R1) to promote human umbilical vein endothelial cells migration and tube formation. *Bioengineered*. 2021;12:2164–2174.
- [26] Ji Y, Ji J, Yin H, et al. Exosomes derived from microRNA-129-5p-modified tumor cells selectively enhanced suppressive effect in malignant behaviors of homologous colon cancer cells. *Bioengineered*. 2021;12:12148–12156.
- [27] Dai T, Liang J, Liu W, et al. The miRNA mir-582-3p suppresses ovarian cancer progression by targeting AKT/MTOR signaling via lncRNA TUG1. *Bioengineered*. 2021;12:10771–10781.
- [28] Yu Y, Wang W, Lu W, et al. Inhibin β -A (INHBA) induces epithelial-mesenchymal transition and accelerates the motility of breast cancer cells by activating the TGF- β signaling pathway. *Bioengineered*. 2021;12:4681–4696.
- [29] Shen C, Tao C, Zhang A, et al. Exosomal microRNA-93-3p secreted by bone marrow mesenchymal stem cells downregulates apoptotic peptidase activating factor 1 to promote wound healing. *Bioengineered*. 2021;13:27–37.
- [30] Cai L, Ye L, Hu X, et al. MicroRNA miR-330-3p suppresses the progression of ovarian cancer by targeting RIPK4. *Bioengineered*. 2021;12:440–449.
- [31] Ge Z, Liu H, Ji T, et al. Long non-coding RNA 00960 promoted the aggressiveness of lung adenocarcinoma via the miR-124a/SphK1 axis. *Bioengineered*. 2021;13:1276–1287.
- [32] Dong S, Chen QL, Song YN, et al. Mechanisms of CCl₄-induced liver fibrosis with combined transcriptomic and proteomic analysis. *J Toxicol Sci*. 2016;41:561–572.
- [33] Zhou L, Wang SB, Chen SG, et al. Prognostic value of ALT, AST, and AAR in hepatocellular carcinoma with B-type hepatitis-associated cirrhosis after radical hepatectomy. *Clin Lab*. 2018;64:1739–1747.
- [34] Abdalla MA, Haj-Ahmad Y. Promising candidate urinary MicroRNA biomarkers for the early detection of hepatocellular carcinoma among high-risk hepatitis C virus egyptian patients. *J Cancer*. 2012;3:19–31.
- [35] Xu F, Liu C, Zhou D, et al. TGF- β /SMAD pathway and its regulation in hepatic fibrosis. *J Histochem Cytochem*. 2016;64:157–167.
- [36] Mu M, Zuo S, Wu RM, et al. Ferulic acid attenuates liver fibrosis and hepatic stellate cell activation via inhibition of TGF- β /Smad signaling pathway. *Drug Des Devel Ther*. 2018;12:4107–4115.
- [37] Lou G, Song X, Yang F, et al. Exosomes derived from miR-122-modified adipose tissue-derived MSCs increase chemosensitivity of hepatocellular carcinoma. *J Hematol Oncol*. 2015;8:122.
- [38] Lou G, Chen L, Xia C, et al. MiR-199a-modified exosomes from adipose tissue-derived mesenchymal stem cells improve hepatocellular carcinoma chemosensitivity through mTOR pathway. *J Exp Clin Cancer Res*. 2020;39:4.
- [39] Nie H, Jiang Z. Bone mesenchymal stem cell-derived extracellular vesicles deliver microRNA-23b to alleviate spinal cord injury by targeting toll-like receptor TLR4 and inhibiting NF- κ B pathway activation. *Bioengineered*. 2021;12:8157–8172.
- [40] Song L, Chen TY, Zhao XJ, et al. Pterostilbene prevents hepatocyte epithelial-mesenchymal transition in fructose-induced liver fibrosis through suppressing miR-34a/Sirt1/p53 and TGF- β 1/Smads signalling. *Br J Pharmacol*. 2019;176:1619–1634.
- [41] Cheng B, Zhu Q, Lin W, et al. MicroRNA-122 inhibits epithelial-mesenchymal transition of hepatic stellate cells induced by the TGF- β 1/Smad signaling pathway. *Exp Ther Med*. 2019;17:284–290.
- [42] Pan WM, Wang H, Zhang XF, et al. miR-210 participates in hepatic ischemia reperfusion injury by forming a negative feedback loop with SMAD4. *Hepatology*. 2020;72:2134–2148.
- [43] Ma N, Li S, Lin C, et al. Mesenchymal stem cell conditioned medium attenuates oxidative stress injury in hepatocytes partly by regulating the miR-486-5p/PIM1 axis and the TGF- β /Smad pathway. *Bioengineered*. 2021;12:6434–6447.